

High-speed liquid lens with 2 ms response and 80.3 nm root-mean-square wavefront error

H. Oku^{a)} and M. Ishikawa

Graduate School of Information Science and Technology, The University of Tokyo, 7-3-1 Hongo, Bunkyo-ku, Tokyo 113-8656, Japan

(Received 31 March 2009; accepted 6 May 2009; published online 2 June 2009)

A liquid lens structure with a step response time of 2 ms, a refractive power range of 52 D, and a root-mean-square (rms) wavefront error of 80.3 nm is reported. This lens uses a liquid-liquid interface with a pinned contact line as a variable refractive surface, and its shape is controlled by a piezostack actuator via a built-in hydraulic amplifier. The measured wavefront error suggests that the method of pinning the contact line to a precise shape is an important factor in achieving higher optical performance. © 2009 The American Physical Society. [DOI: 10.1063/1.3143624]

High-speed focusing technology has been desired for decades. The focusing speed of conventional optical systems is limited by the slow response time involved with the physical actuation of lenses. One possible solution is to develop variable-focus devices that can focus at high-speed by using the electro-optic effect,¹ liquid crystals,^{2–7} and deformation of a refractive surface.^{8–10} Production of practical focusing devices with both high response speed and high optical performance is, however, still a challenge. A liquid interface is known to be suitable for the surface of such a lens due to its almost perfect spherical shape and deformability.^{11–18} Therefore, liquid lenses show great potential to realize both high-speed focusing and high optical performance.^{19–21}

In this letter, a liquid lens using a liquid-liquid interface that can arbitrarily control the focal length in milliseconds and achieve practical imaging performance is reported. This lens dynamically changes the curvature of the interface by means of liquid pressure, as shown in Fig. 1. Two immiscible liquids, indicated as liquids 1 and 2, are infused in two chambers, but they are interfaced at a circular hole that works as

an aperture of the lens. This interface works as a refractive surface due to the different refractive indices of the two liquids. One chamber (the lower chamber in Fig. 1) is equipped with a deformable wall that a piezostack actuator thrusts to change the chamber volume. When the piezostack actuator extends, the lower chamber volume decreases, and the surplus liquid volume presses the interface to change its shape from convex to concave. Since this lens morphs its interface dynamically, it is called a *Dynamorph Lens*.

Although the displacement of the piezostack actuator can be controlled at a frequency on the order of kilohertz, its stroke is quite short, about 10 μm . Since this is too short to achieve a sufficient range of refractive power, a built-in motion amplifier⁹ is used. The area of the deformable wall pressed by the piezostack actuator (S) is much larger than that of the lens surface (s), so that the change in the lens surface shape is approximately S/s times that of the deformable wall.

Based on the above design, a prototype with an aperture diameter of 3.0 mm and a deformable-wall diameter of 24.0 mm was developed. Ultrapure water (refractive index $n_1 = 1.33$) purified by DirectQ-UV (Millipore) and polydimethyl-siloxane (PDMS) ($n_2 = 1.40$) were used as immiscible liquids.

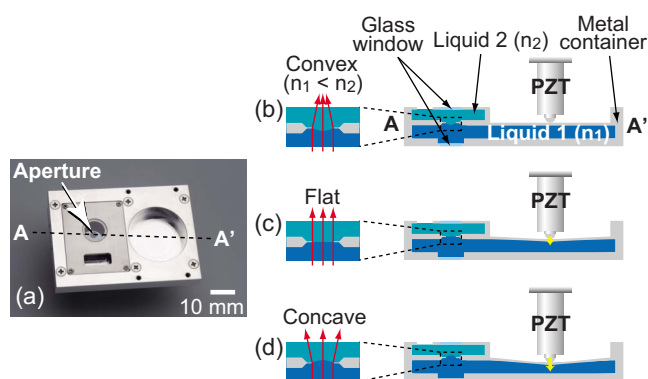


FIG. 1. (Color online) A photograph of the prototype (a) and cross-sectional views to illustrate its focusing mechanism [(b)–(d)]. The small hole at the left in the photograph is the aperture of the lens. The center of the right circular hollow is the point where the piezostack actuator presses. (The piezostack actuator was detached and is not shown in this photograph). Two liquids with refractive indices of n_1 and n_2 are interfaced at the circular aperture shown at the left. Light rays are drawn assuming $n_1 < n_2$.

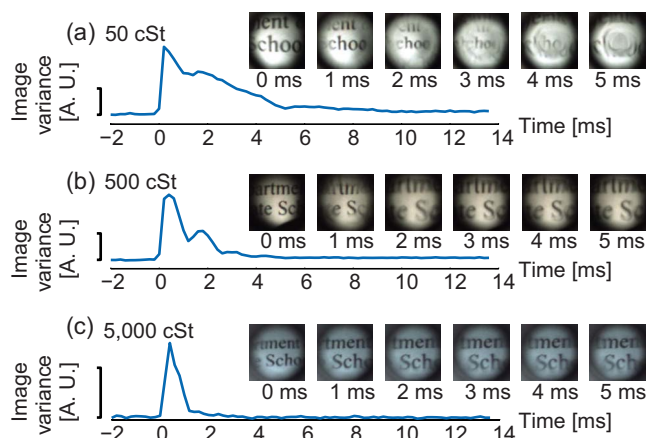


FIG. 2. (Color online) Three kinds of transient responses when the kinematic viscosity of the infused PDMS was 50 (a), 500 (b), and 5000 cSt (c). The profiles of image variance $\sum_x \sum_y |I(x, y; t) - I(x, y; t-1)|$ and captured image sequences are shown, where $I(x, y; t)$ is the intensity of the pixel at (x, y) in t th frame.

^{a)}Electronic mail: hiromasa_oku@ipc.i.u-tokyo.ac.jp.

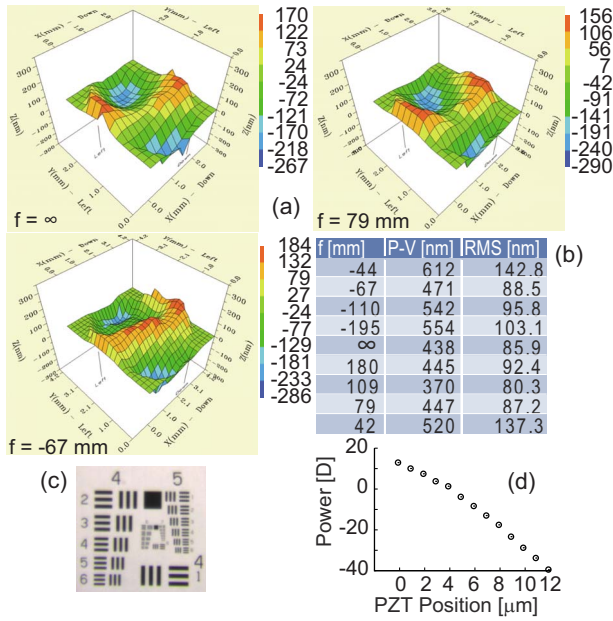


FIG. 3. (Color online) Optical performance of the prototype. Wavefront errors of the prototype [(a) and (b)], image of a resolution chart projected by the prototype (c) and its refractive power range (d).

PDMS is a kind of silicon-based organic polymer, and it is an optically transparent liquid. Its kinematic viscosity depends on the number of repeating monomers, and PDMSs with various kinematic viscosity are commercially available. The available kinematic viscosity ranges from very low [<10 centistokes (cSt)] to very high [$>10^5$ cSt] while its refractive index is almost constant. PDMS was adopted as one liquid so that the relationship between the dynamic behavior of the interface and the liquid's viscosity could be studied.

The radius of the meniscus at the interface needs to be changed quickly. In the case of a liquid lens based on electrowetting, it has been reported that the vibrating interface

behaves like a damped harmonic oscillator.¹⁴ Similar behavior was also observed with our structure. As a preliminary measurement of its transient response depending on the PDMS's viscosity, images obtained through the interface during its transient response were captured using a high-speed camera with a frame rate of 5000 fps.¹⁹ Three kinds of PDMS with different kinematic viscosities of 50, 500, and 5000 cSt were used, together with the ultrapure water. An overdamped response was obtained with the 5000 cSt PDMS [Fig. 2(c)], and image distortion was observed with the 50 and 500 cSt PDMSs [Figs. 2(a) and 2(b), respectively]. Thus, the 5000 cSt PDMS was used for further experiments as described below.

When the two liquids have different densities, the interface will be distorted depending on the direction of gravity. Although this gravity effect can be canceled by using liquids with equal densities,^{12,14} this was not carried out since the density difference between water (0.997 g/cm^3) and PDMS (0.975 g/cm^3) is small.

The pinned contact line should be a well-formed circle in three dimensions to realize a good spherical interface. According to a study on a slightly deformed axisymmetric liquid drop,²² distortions of the interface due to deformation of the contact line exist up to the center of the unperturbed meniscus. Such distortions, however, reduce with distance from the contact line. Assuming that this result is also true for the interface of our lens, the largest deformation of the interface could be limited by the largest contact line deformation. This means that the wavefront error arising from interface deformation can be limited by the precision of the contact line. The deformation of the contact line should be less than one-quarter of the wavelength in the optical path based on the Rayleigh quarter-wave criterion.²³

In the case of the prototype, the acceptable vertical deformation Δ of the contact line parallel to optical axis is $\Delta < (1/4)\lambda / (n_2 - n_1)$, where λ is wavelength. Assuming $\lambda = 546 \text{ nm}$ and $\Delta < 1.95 \text{ }\mu\text{m}$, a machining accuracy of less

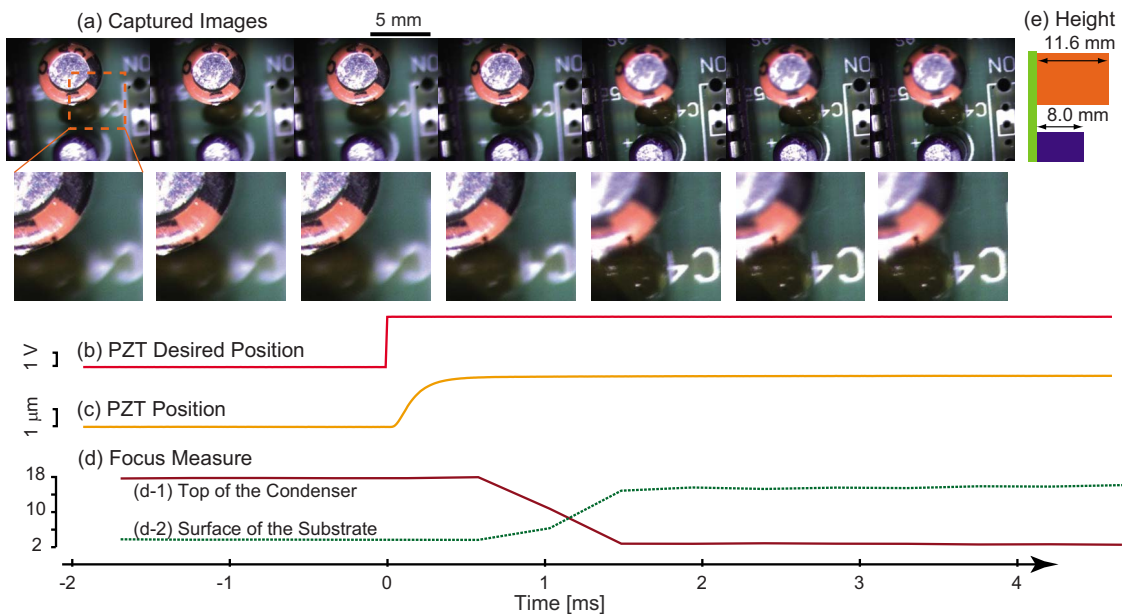


FIG. 4. (Color online) Step response of the prototype. Top image sequence was captured at 2200 fps through the prototype (a). The voltage input to the actuator (b) and the resulting position (c) are shown below. Focus measures of two regions, the top of the capacitor and the substrate, were extracted from the captured images (d). The capacitor was 11.6 mm in height (e).

than 1.95 μm is required for the circular edge pinning the contact line. Photolithography was adopted to fabricate the circular edge to achieve the required accuracy.

Wavefront errors of the prototype were measured with a Shack–Hartmann wavefront sensor with a metal halide lamp. During the measurement, the prototype was placed vertically with the aperture plane parallel to the direction of gravity; that is, the interface deformation due to gravity was maximum. Figure 3(a) shows the wavefront-error distribution at the exit pupil of the lens when its focal length f was -67 mm, ∞ , and 79 mm. Peak-to-valley and root-mean-square (rms) wavefront errors are shown in the table (b). The minimum rms wavefront error was 80.3 nm when f was 109 mm, and the maximum was 142.8 nm when f was -44 mm. This result indicates that the optical performance of the prototype was worse than the required quarter-wave criterion. Excess contact line deformation is suggested as the cause of this, since the measured wavefronts tended to show large error around the periphery of the exit pupil at every focal length. The method of pinning the contact line in a precise shape seems to be important to achieve higher optical performance.

Nevertheless, the prototype achieved sufficient imaging performance for practical use. Figure 3(c) shows a photograph of a USAF 1951 chart captured by a CMOS imager through the prototype with $f=80$ mm and object-side numerical aperture of 0.045. The 71.84 lp/mm bar chart was resolved by the lens.

Figure 3(d) shows how the refractive power depends on the displacement of the piezostack actuator. The refractive power was estimated from the measured positions of an object, the prototype, and the projected image plane. A wide refractive power change of about 52 D was achieved with a displacement of only 12 μm . Note that the initial refractive power could be adjusted by altering the infused volume of liquid 1.

The response time of the prototype was measured to be about 2 ms by capturing high-speed video through the prototype while switching its focal length every 10 ms. An image of a capacitor was captured by a high-speed camera with a frame rate of 2200 fps through the prototype coupled with commercial static lenses. Figure 4(a) shows the captured image sequence from $t=-2$ to 4 ms. The focus was initially at the top of the capacitor at $t=-2$ ms. A $0.01\times$ slow-motion movie of the focus switching is linked to these images (enhanced online).²⁴ A focus switch instruction was input to the piezostack actuator at $t=0$ (b), and it responded in about 0.5 ms (c). The image sequence shows that the focus position started to move farther at about $t=0.6$ ms and reached the substrate at about $t=1.5$ ms. As a measure of focus, the Brenner gradient, $B = \sum_i^N \sum_j^M [I(i,j) - I(i+m,j)]^2$ (Ref. 25) with $m=2$, was adopted. B is a numerical index of the amount of detail included in the digital image. A large B means that the area of the summations included in the calcu-

lation of B is in focus. To show the focus shift quantitatively, two focus measures were calculated for two different areas of the captured image: the top of the capacitor and the substrate. The profile of the focus measures also showed the 1.5 ms response of the focus switching (d). The distance from the substrate to the top of the capacitor was 11.6 mm (e).

In summary, this letter reports a high-speed liquid lens structure driven by a piezostack actuator. The prototype achieved a 2 ms step response time and a minimum rms wavefront error 80.3 nm. The potential applications of this device are axial focus scanning for microscopes, focusing/zooming for camera lenses and machine vision systems, and beam focus control in laser machining and laser trapping.

The authors thank A. Cassinelli for naming the lens structure the Dynamorph Lens. This study was supported under the 2007 Industrial Technology Research Grant Program of the New Energy and Industrial Technology Development Organization (NEDO) of Japan.

- ¹T. Shibaguchi and H. Funato, *Jpn. J. Appl. Phys., Part 1* **31**, 3196 (1992).
- ²J. Eschler, S. Dickmann, and D. A. Mlynski, *Ferroelectrics* **181**, 21 (1996).
- ³M. Hain, R. Glöckner, S. Bhattacharya, D. Dias, S. Stankovic, and T. Tschudi, *Opt. Commun.* **188**, 291 (2001).
- ⁴H. Ren and S. T. Wu, *Appl. Phys. Lett.* **81**, 3537 (2002).
- ⁵H. Ren, Y. H. Fan, and S. T. Wu, *Appl. Phys. Lett.* **83**, 1515 (2003).
- ⁶H. Ren, Y. H. Fan, and S. T. Wu, *Opt. Lett.* **29**, 1608 (2004).
- ⁷B. Wang, M. Ye, and S. Sato, *Opt. Commun.* **250**, 266 (2005).
- ⁸T. Kaneko, T. Ohmi, N. Ohya, N. Kawahara, and T. Hattori, Proceedings of the International Conference on Solid State Sensors and Actuators, Transducers, 1997 (unpublished), Vol. 1, p. 63.
- ⁹H. Oku, K. Hashimoto, and M. Ishikawa, *Opt. Express* **12**, 2138 (2004).
- ¹⁰K. Campbell, Y. Fainman, and A. Groisman, *Appl. Phys. Lett.* **91**, 171111 (2007).
- ¹¹C. B. Gorman, H. A. Biebuyck, and G. M. Whitesides, *Langmuir* **11**, 2242 (1995).
- ¹²B. Berge and J. Peseux, *Eur. Phys. J. E* **3**, 159 (2000).
- ¹³T. Krupenkin, S. Yang, and P. Mach, *Appl. Phys. Lett.* **82**, 316 (2003).
- ¹⁴S. Kuiper and B. H. W. Hendriks, *Appl. Phys. Lett.* **85**, 1128 (2004).
- ¹⁵C. C. Cheng, C. A. Chang, and J. A. Yeh, *Opt. Express* **14**, 4101 (2006).
- ¹⁶H. Ren and S. T. Wu, *Opt. Express* **16**, 2646 (2008).
- ¹⁷C. A. López, C. C. Lee, and A. H. Hirs, *Appl. Phys. Lett.* **87**, 134102 (2005).
- ¹⁸L. Dong, A. K. Agarwal, D. J. Beebe, and H. Jiang, *Nature (London)* **442**, 551 (2006).
- ¹⁹H. Oku and M. Ishikawa, Proceedings of the IEEE LEOS Annual Meeting, 2006 (unpublished), pp. 947–948.
- ²⁰C. A. López and A. H. Hirs, *Nat. Photonics* **2**, 610 (2008).
- ²¹P. M. Moran, S. Dharmatilleke, A. H. Khaw, K. W. Tan, M. L. Chan, and I. Rodriguez, *Appl. Phys. Lett.* **88**, 041120 (2006).
- ²²M. E. R. Shanahan, *J. Phys. D* **22**, 1128 (1989).
- ²³W. J. Smith, *Modern Optical Engineering*, 3rd ed. (McGraw-Hill, New York, 2000), Chap. 11.
- ²⁴See EPAPS supplementary material at <http://dx.doi.org/10.1063/1.3143624> for the $0.01\times$ slow-motion movie of the focus switching.
- ²⁵J. F. Brenner, B. S. Dew, J. B. Horton, T. King, P. W. Neurath, and W. D. Selles, *J. Histochem. Cytochem.* **24**, 100 (1976).